JOURNAL OF COMPUTATIONAL PHYSICS 22, 1–33 (1976)

A First-Order Perturbative Numerical Method for the Solution of the Radial Schrödinger Equation

GH. ADAM[1]

Département de Physique de la Matiere Condensée, Université de Geneve, 32 boulevard d'Yvoy, 1211 Geneve, Suisse

AND

L. GR. IXARU AND A. CORCIOVEI

Institute of Atomic Physics, Section of Theoretical Physics, P. O. Box 5206, Bucharest, Romania

Received August 7, 1975; revised February 10, 1976

A very simple perturbative numerical (PN) algorithm is developed for the solution of the radial Schrödinger equation, using first order perturbation theory along the lines previously developed by Gordon. This algorithm uses the same basic approximation (a step function approximation for the potential well) as that recently reported by Riehl, Diestler, and Wagner (10). It shows, however, an $\mathcal{O}(h^5)$ rate of convergence in the step size h, as compared to the $\mathcal{O}(h^4)$ rate of convergence of the algorithm given in the above cited reference. In the present paper we report a new feature of the PN approach to the solution of the Schrödinger equation, namely, the remarkable stability of the present PN algorithm against the round off errors. A comparison with the Numerov method for eigenvalue problems proves the high efficiency of the present algorithm.

I. INTRODUCTION

When applied to simple quantum systems (e.g., molecules, nuclei), the adiabatic (Born–Oppenheimer) approximation reduces the problem of solving the Schrödinger equation to that of solving the one-dimensional second-order linear equation

$$L(r)\,y(r) = [d^2/dr^2 - f(r)]\,y(r) = 0, \tag{1}$$

$$0 \leqslant r < +\infty, \tag{2}$$

[1] Permanent address: Institute of Atomic Physics, Section of Theoretical Physics, P. O. Box 5206, Bucharest, Romania.

Copyright © 1976 by Academic Press, Inc.
All rights of reproduction in any form reserved.

where

$$f(r) = u(r) - e, \tag{3}$$

$$u(r) = (2\mu/\hbar^2)[V(r) + l(l+1)/r^2], \qquad e = (2\mu/\hbar^2)\,E,$$

with the usual meaning of the parameters.

In the present paper we shall confine our attention to the bound states, which are defined as those solutions of (1) which satisfy the following boundary conditions:

$$y(0) = 0, \tag{4}$$

$$\lim_{r\to\infty} y(r) = 0. \tag{5}$$

The problem (1)–(5) is a singular Sturm–Liouville problem; closed form solutions for eigenvalues and eigenfunctions are available only for a few classes of potentials [1, 2]. It is therefore necessary in general, to look for approximate solutions. Numerical methods for solving (1) can be divided along three different lines: (a) approximate the differential operator d^2/dr^2 by a difference operator and reduce (1) to a set of algebraic equations [3]; (b) approximate the unknown solution $y(r)$, as well as its first order derivative $y'(r)$, by Taylor series [4], or, more generally, develop them in series using a basis of spline functions [5], and evaluate the coefficients of these series by recurrence; (c) approximate the coefficient $f(r)$, (in fact, the reduced potential $u(r)$), by an expression $\bar{f}(r)$, $(\bar{u}(r))$, for which the differential equation can be solved exactly.

The third approach was ignored until the late sixties, when it was finally recognized [6–8] to lead to very efficient algorithms for the solution of (1). Since then, important progress was made on this way [9–13], and several problems of quantum mechanics and of mathematical physics were solved [14–17].

Gordon [6] was the first to go a step further, namely, to exploit *perturbation theory* in order to improve the solution furnished by the alternative (c). However, he insisted upon the piecewise analytic character of the solution, rather than on its perturbative character. This aspect was emphasized only quite recently [9, 10]. Thus, the papers [6–13] propose each a *perturbative numerical method* (PNM, PN method). In fact, two classes of PN methods were investigated. In order to distinguish between them, we shall observe that the perturbative series giving $y(r)$ and $y'(r)$ are *uniquely determined* by the choice of the approximating function $\bar{f}(r)$ $(\bar{u}(r))$. Therefore, a PNM is fully characterized by this choice. Thus, the PN methods reported in references [7–10] are *step function* PN methods (SF–PNM, SF–PN methods), while that reported in references [6, 11] is a *piecewise continuous linear function* PN method (PCLF–PNM).

Comparisons have been reported until now, for scattering problems, between an SF–PNM and the well-known Numerov method [10], and between the PCLF–PNM

of Gordon and the same Numerov method [18]. The authors of these studies conclude that, in general, the Numerov method would be preferable to the PN methods.

In the present paper, our aim is twofold. First, we derive an improved SF–PN algorithm of a remarkable simplicity, which shows, using first-order perturbation theory, an $\mathcal{O}(h^5)$ rate of convergence in the step size h, one order better than that of the SF–PN method of [10]. Second, we compare our algorithm with that produced by the Numerov method for the eigenvalue problem, and prove the existence of a new feature of the perturbative approach, ignored until now. Namely, our investigations in the region of the very small step sizes show a remarkable stability of the computed eigenvalues against the round off errors, in contrast with the instability exhibited by the Numerov method.

The paper is organized as follows. In Section II, we reformulate the numerical problem (1)–(5) so as to deal everywhere with finite quantities only. The principle of implementation of our SF–PNM is discussed in Section III. Then, in Section IV, the first-order perturbative corrections are evaluated and the practical algorithm (33) is written down. The error analysis performed in Section V proves that the rate of convergence of this algorithm is $\mathcal{O}(h^5)$ in the step size h, the maximum possible rate of convergence for this case [13]. Section VI is devoted to practical considerations and to the discussion of the numerical results produced by the present SF–PN method and the Numerov method.

II. Implementation of Singular Sturm–Liouville Problems on Computer

In order to be able to implement an algorithm of the problem (1)–(5), we have to reduce the infinite domain (2) to a *finite* one,

$$[r_0, r_n], \tag{2'}$$

over which the real or complex valued reduced potential function $u(r)$ has *bounded variation.*

First, at $r = 0$, difficulties arise when a singularity occurs in $u(r)$ (e.g., because of the presence of Coulomb and/or centrifugal terms). The standard way for removing them [20], is based on the existence of a convergent power series for $y(r)$ in a neighborhood $[0, r_0]$ of the origin, so that $u(r_0)$ does not overflow the allowable range of the computer. Then, the beginning of the domain (2) is moved from $r = 0$ at $r = r_0$, while the boundary condition (4) is replaced by

$$y(r_0) = y_0, \tag{4'}$$

with y_0 known from the power series expansion.

Second, the infinite right-hand side of the domain (2) has to be replaced by a finite quantity r_n. This problem can be solved in two distinct ways. Canosa [8, 16] and Hajj *et al.* [22] cut the domain (2) at a point r_n' where, in view of (5), the solution $y(r_n')$ becomes "negligible." Tarp [20] and Ixary [21] use the available information about the exponential decrease of the solution $y(r)$ in the asymptotic region, which seems to provide a value r_n sensibly smaller than r_n' (see, e.g., the numerical example investigated in [21]). An important point is, however, obscure in [20, 21], namely, the numerical definition of the asymptotic region. We get an unambiguous definition of it in the following way. For every $e \neq 0$, we write $f(r)$, Eq. (3) in the equivalent form,

$$f(r) = -e[1 - u(r)/e],$$

and observe that as the reduced potential satisfies the boundary condition,

$$\lim_{r \to +\infty} u(r) = 0,$$

the ratio $| u(r)/e |$ can be made smaller than *any* given quantity $\eta > 0$, provided r is large enough. Due to this fact, on a computer with a *t digit binary mantissa*, the difference $1 - u(r)/e$ *equals unity* as long as r reaches a value r_n for which

$$| u(r_n)| < 2^{-t} | e | . \tag{6}$$

As a consequence, for every $r > r_n$, the computed $f(r)$ equals $-e$, and the computed solution shows asymptotic behaviour. Therefore, Eq. (6) provides us with a necessary and sufficient condition for the choice of the finite upper limit r_n of (2'). Of course, if we wish results with a relative accuracy $\eta > 2^{-t}$, the condition (6) can be relaxed to

$$| u(r_n)| < \eta | e | , \qquad \eta \geqslant 2^{-t}. \tag{6'}$$

At $r = r_n$, $y(r_n)$ and $y'(r_n)$ behave as decreasing exponentials, and this provides us with the boundary condition which replaces (5),

$$F(r_n , e) = y'(r_n) + [u(r_n) - e]^{1/2} y(r_n) = 0. \tag{5'}$$

In this way, the original problem (1)–(5) has been put in a form which is suitable for the computer. For the sake of simplicity, we shall use a shooting method [23, 24], and we shall replace the Sturm–Liouville problem by the following *Cauchy problem*:

$$L(r)\, y(r) = 0, \qquad r \in [r_0 , r_n], \tag{7}$$

$$y(r_0) = 0, \qquad y'(r_0) = y_0', \tag{8}$$

where the derivative $y'(r_0)$ is chosen at will; it can be fixed at the end by the condition of normalization of the eigensolutions of (1). The energy values for which (5′) is satisfied will provide us with the eigenvalues of the Sturm–Liouville problem.

III. The Step Function Perturbative Numerical Method

The domain $[r_0, r_n]$ is divided in n arbitrary intervals,

$$[r_{i-1}, r_i] \qquad i = 1, 2, \ldots, n,$$

by the mesh points

$$r_1, r_2, \ldots, r_{n-1}.$$

The solution of the Cauchy problem at the end of the first interval provides us with initial conditions for the second interval, and so on. Therefore, a Cauchy problem is solved within each interval

$$[r_{i-1}, r_i] \qquad i = 1, 2, \ldots, n.$$

As the label i of the interval is immaterial, we shall consider a single interval, of length h, called thereafter $[a, b]$. On this interval, the reduced variable

$$\delta = r - a, \qquad \delta \in [0, h], \tag{9}$$

is introduced, and the Cauchy problem reads

$$L(a + \delta)\, y(a + \delta) = 0, \tag{10}$$

$$y(a) = y_a, \qquad y'(a) = y_a'. \tag{11}$$

In the frame of the perturbative approach, the operator $L(a + \delta)$ is divided into two parts,

$$L(a + \delta) = L_0(a + \delta) - L_1(a + \delta), \tag{12}$$

$$L_0(a + \delta) = d^2/d\delta^2 - \bar{u} + e = d^2/d\delta^2 - \bar{f} \equiv d^2/d\delta^2 - \omega^2, \tag{13a}$$

$$L_1(a + \delta) = u(a + \delta) - \bar{u} \equiv w(\delta), \tag{13b}$$

so that (10) becomes

$$L_0(a + \delta)\, y(a + \delta) = L_1(a + \delta)\, y(a + \delta). \tag{14}$$

A. *Summary of the Zeroth-Order Approximation*

If the right-hand side of Eq. (14) is neglected, the zeroth-order approximation of SF-PNM is obtained. This approximation was fully investigated in [9] and the

results which are of interest for the implementation of perturbative corrections are listed below.

Among the various analytic representations of the solution of the zeroth order, denoted $y^{(0)}(a+\delta)$, the following was proved to be the most suitable for computations:

$$y^{(0)}(a+\delta) = \xi_1(\delta)\, y_a + \delta\xi_2(\delta)\, y_a', \tag{15a}$$

where

$$\xi_1(\delta) = [\exp(\omega\delta) + \exp(-\omega\delta)]/2, \tag{16a}$$

$$\xi_2(\delta) = [\exp(\omega\delta) - \exp(-\omega\delta)]/(2\omega\delta). \tag{16b}$$

From (15a), the first-order derivative is obtained,

$$y^{(0)\prime}(a+\delta) = \omega^2\delta\xi_2(\delta)\, y_a + \xi_1(\delta)\, y_a'. \tag{15b}$$

The *optimal* constant $\bar{u}$, i.e., that $\bar{u}$ for which the errors associated to $y^{(0)}$(b) and $y^{(0)\prime}(b)$ are minimized, is given by [9],

$$\bar{u} = \sum_{m=0}^{\infty} \frac{1}{(m+1)!}\, h^m u^{(m)}(a), \qquad u^{(m)}(a) = d^m u(a)/d\delta^m, \tag{17a}$$

or, equivalently,

$$\bar{u} = (1/h)\int_0^h u(a+\delta)\, d\delta. \tag{17b}$$

The zeroth order approximation results in a second-order method [7–9, 19].

B. *Perturbative Corrections*

Having the solution of the zeroth-order approximation, the original equation (14) can be solved formally by the method of the variation of the constants [25], which yields the same result as that obtained by Gordon [6] via a Wronskian method, namely,

$$y(a+\delta) = \xi_1(\delta)\, p_1(a+\delta) + \delta\xi_2(\delta)\, p_2(a+\delta), \tag{18a}$$

$$y'(a+\delta) = \omega^2\delta\xi_2(\delta)\, p_1(a+\delta) + \xi_1(\delta)\, p_2(a+\delta). \tag{18b}$$

Here, the quantities p_1 and p_2 can be found as perturbative series [6],

$$p_s(a+\delta) = \sum_{k=0}^{\infty} p_s^{(k)}(a+\delta), \qquad s = 1, 2, \tag{19}$$

where the coefficients $p_s^{(k)}$, $s = 1, 2$, are given by

$$p_1^{(0)}(a + \delta) = p_1^{(0)}(a) = y_a\,, \tag{20a}$$

$$p_2^{(0)}(a + \delta) = p_2^{(0)}(a) = y_a'\,, \tag{20b}$$

$$\begin{aligned} p_s^{(k)}(a + \delta) &= (-1)^s \int_0^\delta d\delta_1\, w(\delta_1)\, \delta_1^{2-s} \xi_{3-s}(\delta_1) \\ &\quad \times [\xi_1(\delta_1)\, p_1^{(k-1)}(a + \delta_1) + \delta_1 \xi_2(\delta_1)\, p_2^{(k-1)}(a + \delta_1)], \qquad k = 1, 2,\ldots \end{aligned} \tag{21}$$

If the series (19) are cut at the first-order terms, the zeroth-order approximation (15) is found again. If these series are cut at $p_1^{(k)}$ and $p_2^{(k)}$ respectively, then the first k orders of the perturbative corrections are included in (18). The kth order corrections are given by k-tuple integrals, whose evaluation becomes more and more difficult as k increases. Moreover, the addition of higher order terms is expected to result in a hardly manageable algorithm.

Fortunately, due to the optimal choice (17) for $\bar{u}$, the first order corrections lead to a particularly simple algorithm, Eqs. (33) below, which shows a rate of convergence $\mathcal{O}(h^4)$ over the domain $[r_0\,, r_n]$, the best among *all* the SF-PN algorithms reported until now. (Compare with the rate of convergence $\mathcal{O}(h^2)$ of the zeroth-order approximation of SF-PNM [6, 9, 19, 21], and with the rate of convergence $\mathcal{O}(h^3)$ of the SF-PN algorithm recently reported in [10].)

IV. Evaluation of the First-Order Perturbative Corrections The Practical Algorithm

The addition of the first-order perturbative corrections to the zeroth order approximation of SF-PNM gives,

$$\begin{aligned} y^{(I)}(a + \delta) &= y^{(0)}(a + \delta) + y^{(1)}(a + \delta) = [\xi_1(\delta) + J_1(\delta)]\, y_a \\ &\quad + [\delta \xi_2(\delta) + J_2(\delta)]\, y_a', \end{aligned} \tag{22a}$$

$$\begin{aligned} y'^{(I)}(a + \delta) &= y^{(0)\prime}(a + \delta) + y'^{(1)}(a + \delta) = [\omega^2 \delta \xi_2(\delta) \\ &\quad + J_3(\delta)]\, y_a + [\xi_1(\delta) + J_4(\delta)]\, y_a', \end{aligned} \tag{22b}$$

where,

$$J_1(\delta) = \tfrac{1}{2}\delta^2 D(\delta)\, \xi_2(\delta) - I_2(\delta), \tag{23a}$$

$$J_2(\delta) = 2\delta^3 D(\delta)\, \zeta_0(\delta) + 2K(\delta), \tag{23b}$$

$$J_3(\delta) = \tfrac{1}{2}\delta D(\delta)[\xi_1(\delta) + \xi_2(\delta)] - 2\omega^2 K(\delta), \tag{23c}$$

$$J_4(\delta) = \tfrac{1}{2}\delta^2 D(\delta)\, \xi_2(\delta) + I_2(\delta). \tag{23d}$$

Here we have denoted,

$$D(\delta) = I_1(\delta)/\delta - \bar{u}, \tag{24a}$$

$$K(\delta) = \{I_3(\delta) + [I_1(\delta) - \tfrac{1}{2}\delta u(a+\delta) - \tfrac{1}{2}\delta u(a)]\,\xi_2(\delta)\}/(2\omega)^2. \tag{24b}$$

The quantities I_1, I_2, and I_3 denote the following integrals,

$$I_1(\delta) = \int_0^\delta d\delta_1\, u(a+\delta_1), \tag{25a}$$

$$I_2(\delta) = -(1/2)\int_0^\delta d\delta_1\, u(a+\delta_1)(\delta - 2\delta_1)\,\xi_2(\delta - 2\delta_1), \tag{25b}$$

$$I_3(\delta) = -(1/2)\int_0^\delta d\delta_1\, u'(a+\delta_1)(\delta - 2\delta_1)\,\xi_2(\delta - 2\delta_1). \tag{25c}$$

The function $\zeta_0(\delta)$ is defined in terms of ξ_1 and ξ_2 as follows:

$$\zeta_0(\delta) = [\xi_1(\delta) - \xi_2(\delta)]/(2\omega\delta)^2. \tag{26}$$

Using the Taylor series expansion for $u(a+\delta)$,

$$u(a+\delta) = \sum_{m=0}^{\infty} (1/m!)\,\delta^m u^{(m)}(a), \tag{27}$$

we get after some algebra,

$$D(\delta) = \sum_{m=1}^{\infty} (1/(m+1)!)(\delta^m - h^m)\,u^{(m)}(a), \tag{28}$$

$$I_2(\delta) = C(\delta)\,\zeta_0(\delta) + t^{(1)}(\delta), \qquad K(\delta) = t^{(0)}(\delta), \tag{29}$$

$$C(\delta) = \sum_{m=1}^{\infty} (1/m!)\,\delta^{m+2}u^{(m)}(a) = [u(a+\delta) - u(a)]\,\delta^2, \tag{30}$$

$$t^{(s)}(\delta) = \sum_{p=1}^{\infty} t_p^{(s)}(\delta), \qquad s = 0, 1, \tag{31}$$

$$t_p^{(s)}(\delta) = \sum_{m=0}^{\infty} ((m+p)!/m!(m+2p+1)!)\,u^{(m+2p+s)}(a)\,\delta^{m+2p+3}\zeta_p(\delta), \qquad p = 1, 2, \ldots$$

$$\zeta_1(\delta) = [6\zeta_0(\delta) - (1/2)\,\xi_2(\delta)]/(2\omega\delta)^2, \tag{32a}$$

$$\zeta_{p+2}(\delta) = [2(2p+5)\,\zeta_{p+1}(\delta) + \zeta_p(\delta)]/(2\omega\delta)^2, \qquad p = 0, 1, 2, \ldots \tag{32b}$$

The functions ζ_p are all finite as $|\omega| \to 0$ (see the Appendix).

A considerable simplification of the expressions of y and y', Eqs. (22), is obtained observing, first, that the terms $t^{(s)}(\delta)$ Eq. (31), give high-order contributions (see error analysis in the next section) and can be dropped out without affecting the order of convergence of the numerical method, and second, that at $\delta = h$, $D(h) = 0$. Then, the *initial conditions* for the Cauchy problem on the next interval are given simply by

$$y_1^{(I)}(b) = [\xi_1(h) - C(h)\,\zeta_0(h)]\,y_a + h\xi_2(h)\,y_a', \tag{33a}$$

$$y_1'^{(I)}(b) = \omega^2 h\xi_2(h)\,y_a + [\xi_1(h) + C(h)\,\zeta_0(h)]\,y_a'. \tag{33b}$$

V. Error Analysis

In this section we shall consider the *local truncation errors*

$$T_1^{(I)}(h) = y(b) - y_1^{(I)}(b) = T^{(0)}(h) + C(h)\,\zeta_0(h) \tag{34a}$$

and

$$T_1'^{(I)}(h) = y'(b) - y_1'^{(I)}(b) = T'^{(0)}(h) - C(h)\,\zeta_0(h) \tag{34b}$$

and we shall show that both are $\mathcal{O}(h^5)$, therefore the *order of accuracy* [26, p. 31] of the present SF-PN method is *four*. In (34)

$$T^{(0)}(\delta) = y(a + \delta) - y^{(0)}(a + \delta), \qquad \delta \in [0, h], \tag{35a}$$

and

$$T'^{(0)}(\delta) = y'(a + \delta) - y^{(0)\prime}(a + \delta), \qquad \delta \in [0, h] \tag{35b}$$

are the local truncation errors associated to the zeroth-order approximation of the perturbative approach.

The present error analysis is a straightforward extension of that performed in [9] for the zeroth-order approximation and consists of the following steps.

(i) Leaving undetermined for the moment the quantity $\bar{f} = \bar{u} - e$, Eq. (13a), and using Taylor series about the beginning of the interval $[a, b]$ for the quantities involved in Eq. (35), the local truncation errors $T^{(0)}(\delta)$ and $T'^{(0)}(\delta)$ are evaluated as power series in δ.

(ii) Minimizing the local truncation errors $T^{(0)}(\delta)$ and $T'^{(0)}(\delta)$ with respect to $\bar{f}$ at $\delta = h$ (where initial conditions are produced for the Cauchy problem on the next interval), the expression (17a) is obtained for the step function approximation $\bar{u}$. The quantities $T^{(0)}(h)$ and $T'^{(0)}(h)$ are obtained as power series in h as well [9].

(iii) Expanding in Taylor series the product $C(h)\,\zeta_0(h)$, the local truncation errors (34) are finally obtained:

$$T_1^{(I)}(h) = -[t^{(1)}(h) + h^6\{f_0^2/(2\times 6!) + 5f_1f_2h/(2\times 7!)\}]\,y_a + [2t^{(0)}(h) - f_1^2h^7/(2\times 7!)]\,y_a' + \mathcal{O}(h^8), \tag{36a}$$

$$T_1^{(II)}(h) = -[2f_0t^{(0)}(h) + h^5\{f_1^2/5! + 5f_1f_2\,h/6! + (9f_1f_3 + 25f_2^2/3 + 7f_0f_1^2/2)\,h^2/7!\}]\,y_a + [t^{(1)}(h) + h^6\{f_1^2/(2\times 6!) + 9f_1f_2h/(2\times 7!)\}]\,y_a' + \mathcal{O}(h^8). \tag{36b}$$

Here, $f_m = d^mf(a)/d\delta^m$, $m = 0, 1, 2,...$, while

$$t^{(s)}(h) = -h^5[(f_{2+s} + f_{3+s}\,h/2)/6! + (f_{4+s} + f_0f_{2+s}/2)\,h^2/7!] + \mathcal{O}(h^8), \qquad s = 0, 1 \tag{37}$$

are just the first-order corrections (31) which were dropped out from the practical algorithm (33). Thus, the statement that the order of accuracy of the present SF-PNM is four was proved.

We have to stress the essential role of the error analysis in ensuring a *simple fourth order* PN algorithm. A comparison with the PN algorithm recently reported by Riehl, Diestler, and Wagner (RDW) [10] will best illustrate this point.

(a) In our approach, the step function approximation $\bar{u}$, Eq. (17), is yielded by the error analysis. In [10], $\bar{u}$ is chosen intuitively. In our notation, this choice writes

$$\bar{u}_{\mathrm{RDW}} = u(a + h/2). \tag{38}$$

The perturbative correction $w(\delta)$, Eq. (13b), chosen in [10], can be rewritten in our notations

$$w_{\mathrm{RDW}}(\delta) = (\delta - h/2)\,u'(a + h/2) + (1/2)(\delta - h/2)^2\,u''(a + h/2), \tag{39}$$

where primes indicate derivation with respect to δ. Expanding $\bar{u}_{\mathrm{RDW}}$ and $w_{\mathrm{RDW}}(\delta)$ in Taylor series about the beginning of the interval $[a, b]$, we get for their sum,

$$\bar{u}_{\mathrm{RDW}} + w_{\mathrm{RDW}}(\delta) = u^{(0)}(a) + \delta u^{(1)}(a) + (1/2)\,\delta^2u^{(2)}(a) + (h/48)(12\delta^2 - 6\delta h + h^2)\,u^{(3)}(a) + \cdots, \qquad u^{(m)}(a) = d^mu(a)/d\delta^m, \tag{40}$$

i.e., it coincides with the exact potential $u(a + \delta)$, Eq. (27), in the first three terms only. In contradistinction to this, our first-order perturbative corrections $J_i(\delta)$, Eqs. (23), were evaluated taking for $w(\delta)$ the *exact* expression (13b), with $u(a + \delta)$ given by the infinite Taylor expansion (27). It is this difference which makes the

PN algorithm of [10] to be $\mathcal{O}(h^3)$ on $[r_0, r_n]$ while our PN algorithm is $\mathcal{O}(h^4)$ on $[r_0, r_n]$.

(b) The error analysis helped us to simplify considerably the PN algorithm (33), first, by including higher-order terms in the zeroth-order approximation through $\bar{u}$, and, second, by showing the uselessness of the corrections $t^{(s)}(\delta)$, Eqs. (29), (31), which were dropped out without loss of accuracy. Thus, our algorithm (33) involves a *single* perturbative term, $\pm C(h)\,\zeta_0(h)$, in contradistinction to the PN algorithm of [10] which contains *several* perturbative corrections (see the Appendix of that paper).

(c) For the potentials under investigation in this paper (Section VIA), a very considerable decrease of the computing time was obtained provided the potential related quantities were computed *only once* at a given step size, and then stored (Section VIB). The present PN algorithm requires the storage of *two* quantities, $\bar{u}$, Eq. (17), and $C(h)$, Eq. (30), while the PN algorithm of [10] requires the storage of *three* quantities, $u(a + h/2)$, Eq. (38), $u'(a + h/2)$, and $u''(a + h/2)$, Eq. (39).

We may therefore conclude that our PN algorithm is more efficient than that reported in [10] as it concerns the rate of convergence, the computing time, and the storage area required on computer.

VI. Numerical Results

A. *Reference Eigenvalues*

We have investigated numerically the eigenvalue problem (1)–(5) for the s states of two potentials: the optic potential considered by Bencze [2] and the Morse potential [27]. For both of them analytic expressions exist for the eigenvalues ([2] and [28], respectively).

The optic potential is a sum of Woods–Saxon and derivative Woods–Saxon terms,

$$u(r) = u_0/(1 + t) - (u_0/a_0)\, t/(1 + t)^2, \qquad t = \exp[(r - r_0)/a_0]. \tag{41}$$

Here, u_0, r_0, and a_0 are real or complex adjustable parameters. In the present work we have taken

$$u_0 = -50\ \text{fm}^{-2}, \quad r_0 = 7\ \text{fm}, \quad a_0 = 0.6\ \text{fm}. \tag{42}$$

This potential has 14 bound states, given in Table I with 11 exact decimal figures. These reference eigenvalues have been computed from Bencze's analytic result [2] (which gives the eigenvalues as zeros of the S matrix), in double precision, on an IBM 370/135 computer at the Institute of Atomic Physics, Bucharest, The execution

TABLE I

Reference Eigenvalues for the Optic Potential (41)–(42) Computed from the Analytic Result of Bencze [2]

Eigenvalues (fm^{-2})
$e_0 = -49.457\ 788\ 728$
$e_1 = -48.148\ 430\ 420$
$e_2 = -46.290\ 753\ 954$
$e_3 = -43.968\ 318\ 431$
$e_4 = -41.232\ 607\ 772$
$e_5 = -38.122\ 785\ 096$
$e_6 = -34.672\ 313\ 205$
$e_7 = -30.912\ 247\ 488$
$e_8 = -26.873\ 448\ 915$
$e_9 = -22.588\ 602\ 257$
$e_{10} = -18.094\ 688\ 282$
$e_{11} = -13.436\ 869\ 040$
$e_{12} = -8.676\ 081\ 670\ 4$
$e_{13} = -3.908\ 232\ 480\ 8$

TABLE II

Reference Eigenvalues for the Morse Potential (43), (45), Computed from Eq. (44)

Eigenvalues ($Å^{-2}$)
$e_0 = -178.798\ 538\ 35$
$e_1 = -160.283\ 425\ 63$
$e_2 = -142.780\ 060\ 34$
$e_3 = -126.288\ 442\ 49$
$e_4 = -110.808\ 572\ 07$
$e_5 = -96.340\ 449\ 093$
$e_6 = -82.884\ 073\ 546$
$e_7 = -70.439\ 445\ 434$
$e_8 = -59.006\ 564\ 758$
$e_9 = -48.585\ 431\ 516$
$e_{10} = -39.176\ 045\ 710$
$e_{11} = -30.778\ 407\ 338$
$e_{12} = -23.392\ 516\ 401$
$e_{13} = -17.018\ 372\ 900$
$e_{14} = -11.655\ 976\ 833$
$e_{15} = -7.305\ 328\ 201\ 7$
$e_{16} = -3.966\ 427\ 005\ 1$
$e_{17} = -1.639\ 273\ 243\ 5$
$e_{18} = -.323\ 866\ 916\ 99$

of the program was repeated, in double precision too, on a CDC 3800 computer at the Computing Centre of the University of Geneva, and yielded the results which are given in Table I as well.

The Morse potential [27–30, 22],

$$u(r) = Dt(t - 2), \qquad t = \exp[a(r_e - r)], \tag{43}$$

has the eigenvalues (see, e.g., [28])

$$e_k = -D[1 - aD^{-1/2}(k + \tfrac{1}{2})]^2, \tag{44}$$

which can be easily evaluated to any desired accuracy. Fixing the parameters D, a, and r_e, respectively to

$$D = 188.4355 \text{ Å}^{-2}, \qquad a = 0.711248 \text{ Å}^{-1}, \qquad r_e = 1.9975 \text{ Å}, \tag{45}$$

19 bound states are found, which are given in Table II with 11 exact decimal figures.

B. *Practical Considerations*

The eigenvalue problem (1)–(5) has been implemented on computer, in the manner described in Section II, in FORTRAN IV, both for the present SF-PNM and for the Numerov method. A special subroutine was created for the computation and storage of the mean reduced potential $\bar{u}_i$, Eq. (17), and of the quantities $C_i(h)$, Eq. (30), in the case of the SF-PNM or of the reduced potential $u_i = u(r_i)$ in the case of the Numerov method. In this way, for the two potentials quoted above, a considerable decrease of the computing time was obtained, namely of a factor of about six for the SF-PN method and about five for the Numerov method.

A very important point concerns the formula used in practice to compute the mean reference potential $\bar{u}$. An inspection of the results produced by the error analysis shows that if we really wish to get an $\mathcal{O}(h^5)$ rate of convergence for the PN algorithm (33), we have to keep in the series (17a) *at least* the first four terms. Suitable integration formulae of the equivalent expression (17b) which satisfy to this requirement and use evaluations of $u(r)$ only are the closed Newton–Cotes formulae [25, Section 1.5]. The numerical results reported in this paper have been obtained using the Newton–Cotes formula

$$\begin{aligned}\bar{u} = [19\{u(a) + u(b)\} + 75\{u(a + h/5) + u(b - h/5)\} \\ + 50\{u(a + 2h/5) + u(b - 2h/5)\}]/288,\end{aligned} \tag{46}$$

which coincides with (17a) in the first six terms when developed in power series.

The reduced energy ranges over which the eigenvalues were searched for were

$$[e_{\min}, e_{\max}] = [-50 \text{ fm}^{-2}, -0.2 \text{ fm}^{-2}] \tag{47a}$$

for the optic potential, and

$$[e_{\min}, e_{\max}] = [-180\ \text{Å}^{-2}, -0.2\ \text{Å}^{-2}] \tag{47b}$$

for the Morse potential.

The eigenvalues of the problem (1)–(5) are *simple*. Therefore, the reduced energy range $[e_{\min}, e_{\max}]$, can always be divided in smaller intervals

$$[e_{\min}, e_{\max}] = \sum_k [e_k^{\min}, e_k^{\max}] \tag{48}$$

so that an eigenvalue only exists inside each interval $[e_k^{\min}, e_k^{\max}]$. The shooting procedure used to locate the eigenvalues inside the intervals can be either one-directional (outward) or two-directional with a matching point in the middle. For the solution of the Schrödinger equation, the two-directional shooting is usually recommended (see, e.g., Fox [24] and Cooley [29]). Yet, we used the one-directional outward shooting technique and for both potentials the present SF-PNM produced highly accurate results.

The eigenvalues are produced by bisection: observing that for each interval $[e_k^{\min}, e_k^{\max}]$ entering Eq. (48) the following inequality holds,

$$F(r_n, e_k^{\min})\, F(r_n, e_k^{\max}) < 0, \tag{49}$$

the energy interval $[e_k^{\min}, e_k^{\max}]$ is halved and (49) is used to choose the half-interval containing the eigenvalue, until the condition

$$| e_k^{\max} - e_k^{\min} | \leqslant \eta\, | e_k^{\min} + e_k^{\max} | \tag{50}$$

is fulfilled. Here, η is the relative error which enters Eq. (6′).

The quantities ξ_1, ξ_2, ζ_0, which enter the algorithm (33) are related, in fact to trigonometric or hyperbolic cosine and sine respectively. They make, however, the SF-PNM relatively slow. The method becomes sensibly faster, especially at small step sizes, provided power series are suitably used for these quantities at small values of the product ωh.

The eigenvalues of the potentials (41) and (43) respectively were obtained, in single precision, on an IBM 370/135 computer at the Institute of Atomic Physics, Bucharest, and on a CDC 3800 computer at the Computing Centre of the University of Geneva. On the IBM computer, the relative accuracy in the numerical results, Eqs. (6′) and (50), was required to be

$$\eta = 2^{-20} \simeq 9.5 \times 10^{-7}, \tag{51a}$$

whereas on the CDC computer we have taken

$$\eta = 2^{-35} \simeq 2.92 \times 10^{-11}. \tag{51b}$$

In the following, the results obtained on the CDC computer will be reported, for the better precision (51b) allowed us to give a clear proof of the $\mathcal{O}(h^4)$ rate of convergence of the PN algorithm (33).

C. *Numerical Results and Discussion*

In our computations, we intended, first, to give an experimental proof for the fourth order of accuracy of the SF-PNM which was predicted by the error analysis, and second, to make evident the remarkable constancy of the numerical results produced by the present PN procedure in the limit of the very small step sizes, which is in strong contrast with the behavior of the results produced by the Numerov method. With these aims in mind, we have adopted the easy way of considering equally spaced mesh points for both methods,

$$r_i = r_0 + ih, \qquad i = 1, 2, \ldots, n. \tag{52}$$

In a first version of the numerical program, the asymptotic numerical region was characterized, for all the energy range $[e_{\min}, e_{\max}]$, Eqs. (47), by a single cut off r_n, Eq. (6'), determined from

$$| u(r_n)| \leqslant \eta \mid e_{\max} \mid . \tag{53}$$

The length of the finite domain

$$[r_0 = 0, r_n] \tag{54}$$

was then obtained as a multiple of the step size h (Table III). The Eq. (53) seriously overestimates the numerical asymptotic region for the energies e well below $e_{\max}$, thus leading to useless supplementary computations. A more realistic approximation of the numerical asymptotic region is ensured by the equations

$$| u(r_n(k))| \leqslant \eta \mid e_k^{\max} \mid , \qquad k = 0, 1, 2, \ldots, \tag{55}$$

where the energies $e_k^{\max}$ are defined by Eq. (48). The implementation of the criterion (55) in the numerical program ensured an automatic adjustment of the asymptotic region to each eigenvalue label (Table IV) and resulted in a decrease of the computing time of 10–17 % for both SF-PN and Numerov methods.

Eigenvalues $e_k(l, h; \eta)$ obtained on the CDC 3800 at various step sizes h by means of the present SF-PNM ($l = 1$) and of the Numerov method ($l = 2$) are collected in Tables V to VIII. Besides the eigenvalues the numerical program yielded also the absolute errors

$$\Delta_k(l, h; \eta) = e_k - e_k(l, h; \eta) \tag{56}$$

and the relative errors

$$\epsilon_k(l, h; \eta) = \Delta_k(l, h; \eta)/e_k . \tag{57}$$

TABLE III

The Length r_n of the Domain $[0, r_n]$, Eq. (54), Computed According to the Criterion (53) at Various Step Sizes

h^a	1	$\frac{1}{2}$	$\frac{1}{4}$	$\frac{1}{8}$	$\frac{1}{16}$	$\frac{1}{32}$	$\frac{1}{64}$	$\frac{1}{128}$	$\frac{1}{256}$
r_n for the optic potential	$\frac{25}{1}$	$\frac{49}{2}$	$\frac{97}{4}$	$\frac{194}{8}$	$\frac{388}{16}$	$\frac{775}{32}$	$\frac{1550}{64}$	$\frac{3099}{128}$	$\frac{6198}{256}$
r_n for the Morse potential	$\frac{47}{1}$	$\frac{92}{2}$	$\frac{184}{4}$	$\frac{367}{8}$	$\frac{733}{16}$	$\frac{1465}{32}$	$\frac{2928}{64}$	$\frac{5855}{128}$	$\frac{11,709}{256}$

[a] The step size h and the length r_n are measured in fermis for the optic potential (41)–(42), and in Ångstroms for the Morse potential (43), (45).

TABLE IV

Variation of the Length r_n of the Domain $[0, r_n]$, Eq. (54), with the Eigenvalue Label when Computed according to the criterion (55)[a]

Eigenvalue label	0	1	2	3	4	5	6	7	8
r_n for the optic potential	5354	5357	5363	5374	5381	5393	5410	5429	5451
r_n for the Morse potential	9265	9303	9346	9389	9438	9487	9544	9601	9662

9	10	11	12	13	14	15	16	17	18
5477	5508	5558	5632	5783	—	—	—	—	—
9737	9811	9906	10001	10110	10267	10430	10734	11130	11709

[a] Values obtained at the step size $h = 1/256$. Results are given in units h.

TABLE V

Some of the Eigenvalues Produced by the Present SF-PNM, on the Computer CDC 3800, for the Optic Potential (41)–(42). Absolute Errors, Eq. (56), are Given in Parantheses as Yielded by the Computer

h	e_0	e_1	e_2
1	−49.457 824 948 (36 222)	−48.140 665 367 (−7 765 052)	−46.261 311 078 (−29 442 876)
1/2	−49.457 793 813 (5 085)	−48.147 904 495 (−525 924)	−46.288 499 895 (−2 254 059)
1/4	−49.457 789 108 (381)	−48.148 397 092 (33 327)	−46.290 606 025 (147 929)
1/8	−49.457 788 753 (25)	−48.148 428 330 (−2 089)	−46.290 744 399 (−9 355)
1/16	−49.457 788 729 (3)	−48.148 430 289 (− 129)	−46.290 753 369 (− 586)
1/32	−49.457 788 728 (1)	−48.148 430 410 (−8)	−46.290 753 918 (−36)
1/64	−49.457 788 728 (1)	−48.148 430 419 (1)	−46.290 753 951 (−3)
1/128	−49.457 788 728 (1)	−48.148 430 419 (1)	−46.290 753 953 (−1)
1/256	−49.457 788 728 (1)	−48.148 430 419 (1)	−46.290 753 955 (1)
1/512	−49.457 788 728 (1)	−48.148 430 419 (1)	−46.290 753 955 (1)

h	e_6	e_7	e_8
1	−34.387 609 285 (−284 703 921)	−30.777 641 642 (−134 605 846)	−26.916 460 263 (43 011 348)
1/2	−34.647 552 607 (−24 760 597)	−30.879 676 489 (−32 570 998)	−26.833 752 744 (−39 696 171)
1/4	−34.670 336 790 (−1 976 414)	−30.909 476 468 (−2 771 019)	−26.869 823 491 (−3 625 424)
1/8	−34.672 181 651 (− 131 554)	−30.912 059 798 (− 187 689)	−26.873 198 490 (− 250 426)

TABLE V (*continued*)

h	e_6	e_7	e_8
1/16	−34.672 304 852 (−8 353)	−30.912 235 517 (−11 970)	−26.873 432 864 (−16 052)
1/32	−34.672 312 681 (− 524)	−30.912 246 735 (− 753)	−26.873 447 905 (−1 010)
1/64	−34.672 313 172 (−33)	−30.912 247 440 (−48)	−26.873 448 853 (−63)
1/128	−34.672 313 204 (−1)	−30.912 247 484 (−4)	−26.873 448 911 (−4)
1/256	−34.672 313 204 (−1)	−30.912 247 486 (−1)	−26.873 448 915 (0)
1/512	−34.672 313 206 (1)	−30.912 247 489 (2)	−26.873 448 917 (1)

h	e_{11}	e_{12}	e_{13}
1	−12.797 804 055 (−639 064 985)	−8.406 952 076 1 (−269 129 594 3)	−4.338 717 870 9 (430 485 390 0)
1/2	−13.395 408 026 (−41 461 014)	−8.619 235 031 8 (−56 846 638 7)	−3.898 413 425 8 (−9 819 055 1)
1/4	−13.431 217 846 (−5 651 194)	−8.670 346 557 6 (−5 735 112 8)	−3.902 972 226 3 (−5 260 254 6)
1/8	−13.436 446 940 (− 422 100)	−8.675 636 700 8 (− 444 969 6)	−3.907 802 612 3 (− 429 868 6)
1/16	−13.436 841 439 (−27 600)	−8.676 052 298 9 (−29 371 6)	−3.908 203 750 7 (−28 730 1)
1/32	−13.436 867 294 (−1 746)	−8.676 079 808 3 (−1 862 2)	−3.908 230 653 8 (−1 827 0)
1/64	−13.436 868 930 (−110)	−8.676 081 552 6 (− 117 8)	−3.908 232 365 6 (−115 3)
1/128	−13.436 869 032 (−8)	−8.676 081 662 1 (−8 4)	−3.908 232 472 4 (−8 5)
1/256	−13.436 869 038 (−2)	−8.676 081 668 1 (−2 3)	−3.908 232 479 7 (−1 2)
1/512	−13.436 869 039 (−1)	−8.676 081 670 4 (0)	−3.908 232 479 9 (− 9)

TABLE VI

Eigenvalues Produced for the Same Potential by the Numerov Method

h	e_0	e_1	e_2
1/4	−49.457 792 541	−48.148 516 677	−46.291 382 801
	(3 814)	(86 258)	(628 847)
1/8	−49.457 788 967	−48.148 435 788	−46.290 792 966
	(239)	(5 369)	(39 012)
1/16	−49.457 788 747	−48.148 430 759	−46.290 756 391
	(20)	(340)	(2 437)
1/32	−49.457 788 739	−48.148 430 461	−46.290 754 118
	(12)	(42)	(165)
1/64	−49.457 788 769	−48.148 430 461	−46.290 754 002
	(42)	(42)	(48)
1/128	−49.457 788 892	−48.148 430 568	−46.290 754 098
	(165)	(150)	(144)
1/256	−49.457 789 414	−48.148 431 135	−46.290 754 621
	(686)	(716)	(668)
1/512	−49.457 791 609	−48.148 433 078	−46.290 756 166
	(2 882)	(2 659)	(2 212)

h	e_6	e_7	e_8
1/4	−34.715 357 745	−30.995 496 921	−27.021 562 100
	(43 044 540)	(83 249 434)	(148 113 185)
1/8	−34.674 930 910	−30.917 277 758	−26.882 336 402
	(2 617 705)	(5 030 271)	(8 887 487)
1/16	−34.672 475 677	−30.912 559 177	−26.873 998 627
	(162 472)	(311 690)	(549 712)
1/32	−34.672 323 355	−30.912 266 937	−26.873 483 190
	(10 150)	(19 450)	(34 275)

TABLE VI (*continued*)

h	e_6	e_7	e_8	
1/64	−34.672 313 899 (694)	−30.912 248 744 (1 256)	−26.873 451 095 (2 180)	
1/128	−34.672 313 420 (215)	−30.912 247 696 (209)	−26.873 449 241 (326)	
1/256	−34.672 313 879 (673)	−30.912 247 989 (502)	−26.873 449 551 (636)	
1/512	−34.672 315 937 (2 732)	−30.912 250 195 (2 708)	−26.873 451 421 (2 506)	
h	e_{11}	e_{12}	e_{13}	
1/4	−14.012 672 983 (575 803 943)	−9.492 509 507 1 (816 427 836 7)	−5.002 697 955 4 (1.094 465 474 5)	−0.677 (spurious)
1/8	−13.470 554 122 (33 685 082)	−8.723 295 495 4 (47 213 824 9)	−3.970 499 419 1 (62 266 938 3)	
1/16	−13.438 939 919 (2 070 879)	−8.678 977 610 1 (2 895 939 6)	−3.912 041 879 7 (3 809 398 9)	
1/32	−13.436 997 948 (128 908)	−8.676 261 834 3 (180 163 9)	−3.908 469 335 6 (236 854 8)	
1/64	−13.436 877 127 (8 087)	−8.676 092 962 3 (11 291 8)	−3.908 247 313 9 (14 833 1)	
1/128	−13.436 869 709 (669)	−8.676 082 563 1 (892 7)	−3.908 233 613 2 (1 132 4)	
1/256	−13.436 869 800 (760)	−8.676 082 419 7 (749 2)	−3.908 233 294 7 (813 9)	
1/512	−13.436 871 344 (2 304)	−8.676 084 654 9 (2 984 4)	−3.908 235 503 8 (3 023 0)	

TABLE VII

Some of the Eigenvalues Produced by the Present SF-PNM, on the Computer CDC 3800, for the Morse Potential (43), (45). Absolute Errors, Eq. (56), are Given in Parantheses as Yielded by the Computer

h	e_0	e_1	e_2
1	−170.670 815 53	−152.816 310 06	−131.171 864 06
	(−8.127 722 81)	(−7.467 115 57)	(−11.608 196 28)
1/2	−178.109 506 50	−159.100 691 43	−141.669 308 54
	(−689 031 85)	(−1.182 734 20)	(−1.110 751 81)
1/4	−178.748 202 27	−160.152 906 51	−142.599 626 95
	(−50 336 09)	(−130 519 11)	(−180 433 39)
1/8	−178.795 178 78	−160.274 014 89	−142.765 950 55
	(−3 359 56)	(−9 410 74)	(−14 109 79)
1/16	−178.798 324 90	−160.282 815 84	−142.779 126 52
	(− 213 45)	(− 609 79)	(− 933 83)
1/32	−178.798 524 96	−160.283 387 18	−142.780 001 14
	(−13 39)	(−38 45)	(−59 20)
1/64	−178.798 537 51	−160.283 423 22	−142.780 056 63
	(− 83)	(−2 41)	(−3 71)
1/128	−178.798 538 30	−160.283 425 48	−142.780 060 11
	(−4)	(− 15)	(− 23)
1/256	−178.798 538 35	−160.283 425 62	−142.780 060 33
	(0)	(−1)	(−1)
1/320	−178.798 538 36	−160.283 425 63	−142.780 060 34
	(1)	(0)	(0)

h	e_7	e_8	e_9
1	−72.080 957 568	−59.018 884 891	−48.907 424 317
	(1.651 512 133)	(12 320 133)	(321 992 802)
1/2	−68.150 454 517	−56.854 593 577	−47.184 817 221
	(−2.288 990 917)	(−2.151 971 181)	(−1.400 614 295)
1/4	−70.220 633 869	−58.792 524 833	−48.384 968 629
	(−218 811 566)	(−214 039 925)	(−200 462 887)
1/8	−70.416 512 862	−58.983 954 312	−48.563 625 034
	(−22 932 572)	(−22 610 446)	(−21 806 482)
1/16	−70.437 787 998	−59.004 907 986	−48.583 813 590
	(−1 657 436)	(−1 656 772)	(−1 617 925)
1/32	−70.439 337 965	−59.006 456 948	−48.585 325 895
	(− 107 469)	(− 107 809)	(− 105 621)
1/64	−70.439 438 656	−59.006 557 950	−48.585 424 842
	(−6 778)	(−6 807)	(−6 674)
1/128	−70.439 445 011	−59.006 564 332	−48.585 431 098
	(− 423)	(− 426)	(− 417)
1/256	−70.439 445 410	−59.006 564 730	−48.585 431 490
	(−24)	(−27)	(−26)
1/320	−70.439 445 425	−59.006 564 749	−48.585 431 507
	(−9)	(−8)	(−9)

TABLE VII (*continued*)

h	e_{11}	e_{12}	e_{13}
1	−31.728 230 206 (949 822 868)	−24.303 395 312 (910 878 911)	−18.776 196 156 (1.757 823 256)
1/2	−30.698 952 713 (−79 454 625)	−23.603 254 889 (210 738 488)	−17.417 297 022 (398 924 122)
1/4	−30.651 969 946 (−126 437 392)	−23.300 086 926 (−92 429 476)	−16.942 679 621 (−75 693 279)
1/8	−30.759 384 130 (−19 023 207)	−23.375 356 405 (−17 159 997)	−17.003 323 364 (−15 049 536)
1/16	−30.776 965 664 (−1 441 674)	−23.391 204 489 (−1 311 913)	−17.017 213 618 (−1 159 282)
1/32	−30.778 312 700 (−94 638)	−23.392 430 083 (−86 318)	−17.018 296 475 (−76 425)
1/64	−30.778 401 350 (−5 988)	−23.392 510 936 (−5 465)	−17.018 368 059 (−4 841)
1/128	−30.778 406 961 (− 376)	−23.392 516 058 (− 343)	−17.018 372 596 (− 304)
1/256	−30.778 407 315 (−23)	−23.392 516 380 (−21)	−17.018 372 880 (−20)
1/320	−30.778 407 329 (−8)	−23.392 516 392 (−9)	−17.018 372 894 (−5)

h	e_{16}	e_{17}	e_{18}
1	−4.510 719 020 9 (544 292 015 7)	−2.022 165 515 9 (382 892 272 4)	−0.494 954 823 11 (171 087 906 11)
1/2	−4.175 132 365 7 (208 705 360 5)	−1.771 794 866 4 (132 521 622 8)	−0.382 314 537 65 (58 447 620 66)
1/4	−3.911 096 833 8 (−55 330 171 3)	−1.600 316 312 3 (−38 956 931 2)	−0.305 824 068 10 (−18 042 848 90)
1/8	−3.958 768 976 5 (−7 658 028 6)	−1.634 307 529 5 (−4 965 714 1)	−0.321 650 899 41 (−2 216 017 59)
1/16	−3.965 827 843 2 (−599 161 9)	−1.638 883 567 8 (− 389 675 7)	−0.323 692 596 63 (− 174 320 36)
1/32	−3.966 387 344 5 (−39 660 5)	−1.639 247 430 5 (−25 813 1)	−0.323 855 364 11 (−11 552 88)
1/64	−3.966 424 490 1 (−2 515 0)	−1.639 271 606 2 (−1 637 3)	−0.323 866 184 19 (− 732 81)
1/128	−3.966 426 847 0 (− 158 0)	−1.639 273 140 9 (− 102 6)	−0.323 866 870 99 (−46 00)
1/256	−3.966 426 995 1 (−10 0)	−1.639 273 236 8 (−67 5)	−0.323 866 914 10 (−2 90)
1/320	−3.966 427 001 5 (−3 5)	−1.639 273 241 0 (−2 5)	−0.323 866 915 99 (−1 00)

TABLE VIII

Eigenvalues Produced for the Same Potential by the Numerov Method

h	e_0	e_1	e_2
1/8	−178.800 305 91 (1 765 61)	−160.294 355 29 (10 929 66)	−142.814 490 43 (34 430 09)
1/16	−178.798 647 03 (108 68)	−160.284 094 54 (668 91)	−142.782 155 56 (2 095 22)
1/32	−178.798 545 14 (6 79)	−160.283 467 23 (41 60)	−142.780 190 48 (130 14)
1/64	−178.798 538 80 (45)	−160.283 428 26 (2 63)	−142.780 068 52 (8 17)
1/128	−178.798 538 48 (13)	−160.283 425 97 (34)	−142.780 061 02 (68)
1/256	−178.798 538 77 (42)	−160.283 426 18 (55)	−142.780 061 01 (66)
1/320	−178.798 539 12 (77)	−160.283 426 70 (1 07)	−142.780 061 46 (1 12)

h	e_7	e_8	e_9
1/8	−70.831 786 699 (392 341 265)	−68.415 ... (spurious)	 (spurious)
1/16	−70.462 453 157 (23 007 723)	−59.034 573 641 (28 008 883)	−48.617 779 851 (32 348 335)
1/32	−70.440 864 563 (1 419 129)	−59.008 290 210 (1 725 453)	−48.587 421 939 (1 990 423)
1/64	−70.439 533 907 (88 474)	−59.006 672 287 (107 530)	−48.585 555 492 (123 976)
1/128	−70.439 451 120 (5 687)	−59.006 571 650 (6 893)	−48.585 439 402 (7 886)
1/256	−70.439 446 494 (1 060)	−59.006 565 647 (889)	−48.585 432 653 (1 136)
1/320	−70.439 446 326 (892)	−59.006 566 040 (1 282)	−48.585 432 783 (1 267)

TABLE VIII (*continued*)

h	e_{11}	e_{12}	e_{13}
1/16	−30.815 990 889 (37 583 550)	−23.430 448 876 (37 932 475)	−17.054 934 234 (36 561 335)
1/32	−30.780 714 902 (2 307 564)	−23.394 843 134 (2 326 733)	−17.020 613 494 (2 240 594)
1/64	−30.778 551 013 (143 676)	−23.392 661 245 (144 843)	−17.018 512 346 (139 446)
1/128	−30.778 416 480 (9 142)	−23.392 525 649 (9 248)	−17.018 381 743 (8 843)
1/256	−30.778 408 403 (1 065)	−23.392 517 660 (1 259)	−17.018 374 150 (1 250)
1/320	−30.778 408 457 (1 119)	−23.392 517 807 (1 405)	−17.018 374 184 (1 284)

h	e_{16}	e_{17}	e_{18}
1/16	−3.988 882 198 9 (22 455 193 9)	−1.654 335 958 8 (15 062 715 2)	−0.330 741 531 83 (6 874 614 83)
1/32	−3.967 799 567 0 (1 372 562 0)	−1.640 192 832 8 (919 589 2)	−0.324 285 328 56 (418 411 57)
1/64	−3.966 512 406 2 (85 401 2)	−1.639 330 467 0 (57 223 4)	−0.323 892 962 19 (26 045 19)
1/128	−3.966 432 450 8 (5 445 7)	−1.639 276 969 5 (3 726 0)	−0.323 868 674 37 (1 757 38)
1/256	−3.966 427 917 9 (968 1)	−1.639 274 108 2 (864 7)	−0.323 867 608 68 (691 68)
1/320	−3.966 428 151 4 (1 146 3)	−1.639 274 391 2 (1 147 6)	−0.323 867 764 32 (847 33)

In Tables V–VIII, the numbers given under parantheses are the absolute errors $\Delta_k(l, h; \eta)$. A violation of Eq. (56), of ± 1 on the 11th decimal figure, which is sometimes observed, is due to the I/O errors associated with the I/O operations READ for e_k and PRINT for $e_k(l, h; \eta)$.

Plots of the moduli of the relative errors $\epsilon_k(l, h; \eta)$, Eq. (57), are given in Figs. 1–4, versus the eigenvalue label k and the step size density $1/h$. These plots provide us with very suggestive three-dimensional maps from which we can made inferences about the possibilities offered by each numerical method, SF-PN or Numerov.

By fixing one of the three parameters which enter these maps, we get three important functional dependences which provide us with information about the two methods under consideration.

(1) *Error (accuracy) versus mesh density at constant eigenvalue label.* This functional dependence provides us with information about the rate of convergence (order of accuracy) which is experimentally obtained for each method. Indeed, the absolute errors can be written as

$$\Delta_k(l, h; \eta) = T_k(l, h) + R_k(l, h; \eta), \tag{58}$$

where $T_k(l, h)$ denotes the accumulated discretization (truncation) error, while $R_k(l, h; \eta)$ denotes the accumulated round off error. According to the error analysis, a behavior

$$T_k(l, h) \to h^4 \qquad \text{as } h \to 0 \tag{59}$$

is expected for both SF-PN and Numerov methods. At step sizes large enough, $R_k(l, h; \eta) \ll T_k(l, h)$, therefore a h^4 behavior of $\Delta_k(l, h; \eta)$ should be observed over some step size range. This is indeed the case in the Fig. 1–4, therefore an experimental proof was given for the fourth-order of accuracy of the present SF-PN method, as well as for the Numerov method.

The behavior of the results produced by the two methods is, however, different at *very large* and at *very small* step sizes. The deviation of each numerical eigenvalue $e_k(2, h; \eta)$ from the exact eigenvalues e_k is seen to increase with the step size h according to the $\mathcal{O}(h^4)$ law, *always keeping the same sign*, until the Numerov method becomes unable to yield the eigenvalue correctly. Now, the deviation of the numerical eigenvalue $e_k(1, h; \eta)$ from the exact eigenvalue e_k is seen to increase with the step size as well. However, for step sizes larger than some threshold $h = h(k)$, this deviation *changes the sign* and the $\mathcal{O}(h^4)$ law is no more satisfied (see Tables V and VII and Figs. 1 and 3). This feature of the PN methods ensures good results even for very few mesh points, and was often quoted in the past [6–8, 11, 21] as the main advantage of the perturbative approach over the finite-difference

approach. Let us remark that because of this feature of the PN approach, the six decimal accuracy of the IBM computer was exhausted before we could get a clear confirmation of the $O(h^4)$ law of convergence of the present SF-PN method.

An interesting and yet unexplored region (in connection with the perturbative methods) is that of the *very small step sizes*, where the limitations imposed by the finite length mantissa of the computer become essential. As it is clearly seen from Tables VI and VIII, and from Figs. 2 and 4, the finite length mantissa of the com-

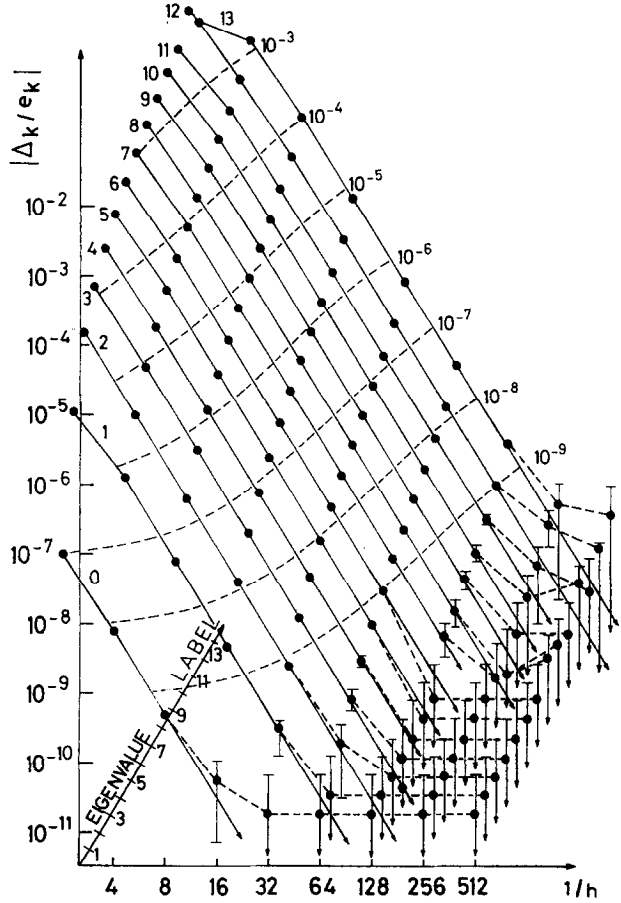

FIG. 1. Graphical representation of the eigenvalue spectrum yielded by the present SF-PNM for the optic potential (41)–(42). The moduli of the relative errors ϵ_k, Eq. (57), are plotted against the eigenvalue label k and the mesh points density $1/h$. Each solid line joins the results obtained at various step sizes for a same eigenvalue. The vertical segments give the computer induced uncertainities (60). In their region, the solid lines are continued by dashed lines. Otherwise, dashed lines join the results of equal accuracy specified on the diagram.

puter results in the *instability* of the Numerov method at very small step sizes. As long as the truncation error term $T_k(2, h)$ is dominant in Eq. (58), the absolute/relative error decreases as the step size h decreases. At smaller step sizes, however, the round off error term $R_k(2, h; \eta)$ becomes dominant. Its growth with the mesh density $1/h$ produces the very illustrative "valley shape" shown by the Figs. 2 and 4. The use of a two-directional shooting procedure [24, 29] leads to a decrease of the accumulated round off errors, but it does *not* supress it.

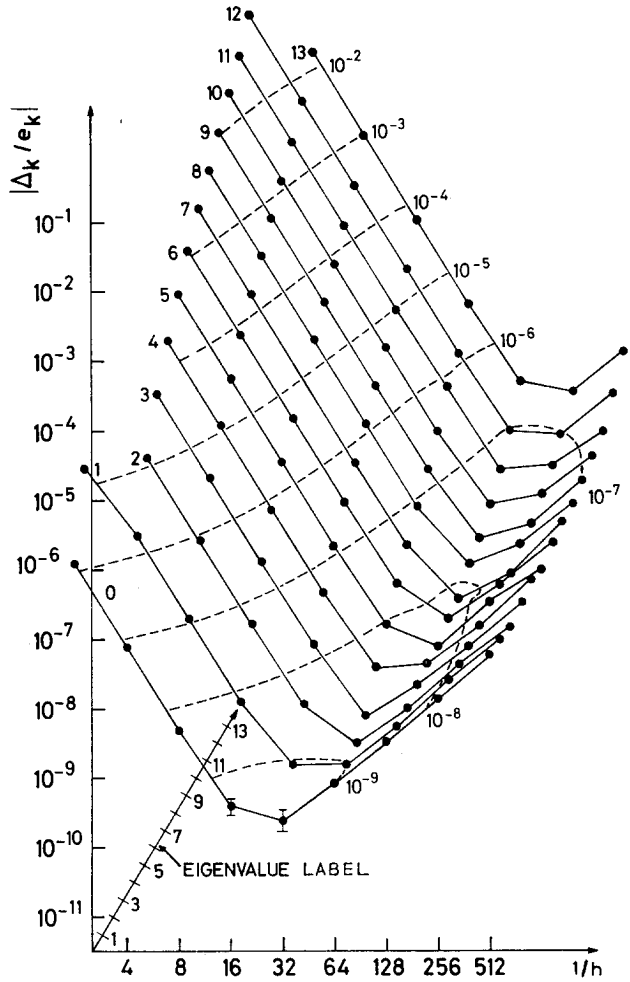

FIG. 2. The same graphical representation of the numerical results as in Fig. 1, showing the eigenvalue spectrum yielded by the Numerov method for the optic potential (41)–(42).

The picture offered by the present SF-PNM at very small step sizes is completely different from that of the Numerov method. Over all the investigated step sizes, for all eigenvalues, and on both computers, we *have not observed any accumulation of the round off errors* in the eigenvalues produced by the PN algorithm (33). From Tables V and VII and from Figs. 1 and 3, we see that the eigenvalues produced by the present SF-PNM converge uniformly towards the reference eigenvalues until the available figures on computer are exhausted, and then *remain constant* within an error

$$\pm(2\eta e_k(l, h; \eta) + \text{one unit on the 11th decimal place of } e_k(l, h; \eta)). \quad (60)$$

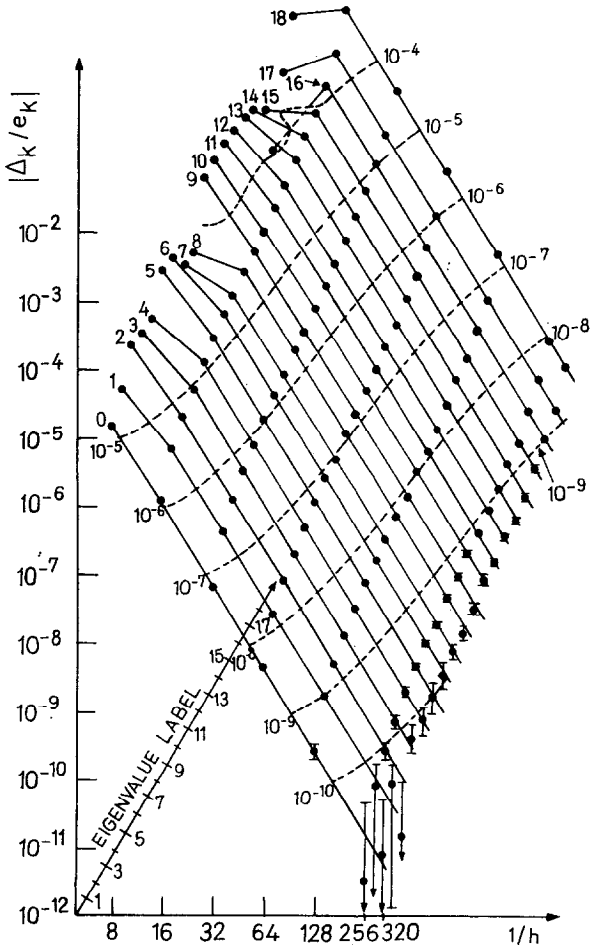

FIG. 3. The same graphical representation of the numerical results as in Fig. 1, showing the eigenvalue spectrum yielded by the present SF-PNM for the Morse potential (43), (45).

This is an inherent, computer induced, uncertainity in the results which appears to be very important for the present SF-PNM (Figs. 1 and 3, where its magnitude, given by the length of the vertical lines, is seen to prevail over the absolute error (56) at very small step sizes), while of negligible importance for the Numerov method (Figs. 2 and 4).

The fact that we have got the same behavior of the PN results for two different potentials, undoubtedly shows that a new feature of the SF-PNM was put in evidence. The theoretical investigation of this point will be performed in a forthcoming paper.

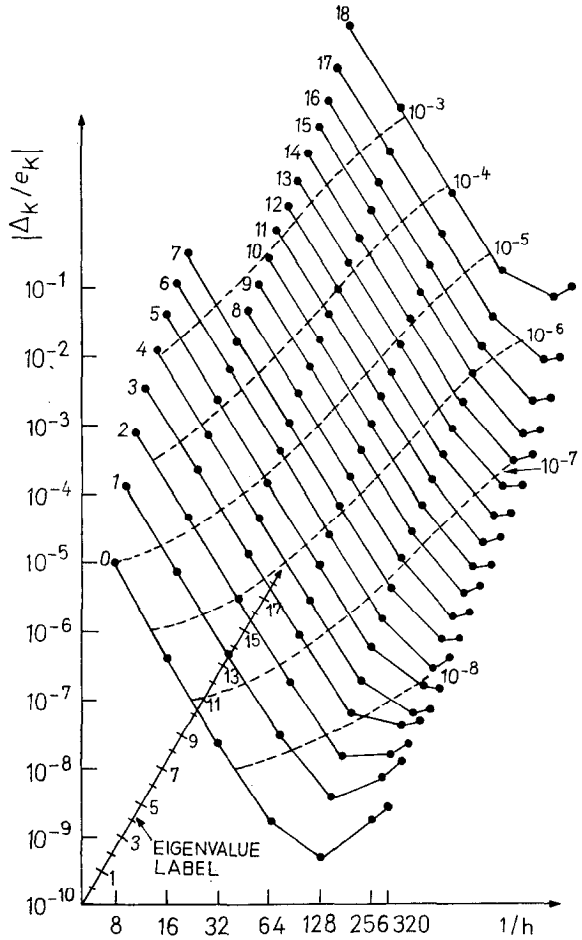

FIG. 4. The same graphical representation of the numerical results as in Fig. 1, showing the eigenvalue spectrum yielded by the Numerov method for the Morse potential (43), (45).

(2) *Error (accuracy) versus eigenvalue label at constant step size, and*

(3) *Mesh density versus eigenvalue label at constant accuracy.*

These functional dependences provide us with information about the uniformity of approximation of the eigenvalue spectrum by each method. In this respect, the trends of the two methods are comparable. Each yields the best results for the fundamental eigenstate. As the eigenvalue label increases, the mesh density needed to ensure the same accuracy increases. However, this increase is sensibly smaller for the SF-PNM than for the Numerov method.

Let us consider now another important parameter, *the computing time.* As already mentioned at the beginning of Section VIC, we were not essentially [illegible] puting time by implementing variable step sizes like in references [6] and [10]. Therefore, the present PN data for the computing time are to be considered as *maximum values.* At present, we are not in a position to estimate how efficient the PN algorithm (33) would become when implementing variable step sizes.

On the CDC 3800 computer, the library subroutine TIMEZB yielded, within 1 msec, the computing time required by each method to get the eigenvalue spectrum at a given step size h. Comparing data at the same step size for two completely different methods such as PN and Numerov, is, however, insignificant. The parameter which is convenient for such a comparison is *the computing time at constant accuracy.* We have got it as follows. The total computing time at the step size h was divided between the eigenvalues e_k proportionally to the lengths $r_n(k)$, Eq. (55), of the numerical domains of the equation for every eigenvalue. The knowledge of the times per eigenvalue allowed us to estimate the total computing time needed to obtain a given accuracy over all the eigenvalue spectrum (i.e., to get the eigenvalue spectrum along the lines of constant accuracy in Figs. 1–4). Data are collected in Table IX.

The reported data illustrate very well the importance of the use of power series for the computation of the quantities ξ_1, ξ_2, ζ_0, mentioned in Section VIB in connection with the PN algorithm (33). While the Numerov method requires the same computing time per step, irrespective of the step size, the abovementioned use of power series clearly ensures a decrease of the computing time per step of the present SF-PNM when the step size decreases. This remarkable fact is responsible for the general trend shown by the ratio $t_{\mathrm{NM}}/t_{\mathrm{SF-PNM}}$ of increasing with the accuracy.

The dependence of the ratio $t_{\mathrm{NM}}/t_{\mathrm{SF-PNM}}$ on the shape of the potential well, previously reported for the scattering problem by Riehl, Diestler, and Wagner [10], is confirmed for the eigenvalue problem as well. For the optic potential, which is negative and flat at the origin, the Numerov method is a little faster up to accuracies $\epsilon = 10^{-5}$. For $\epsilon = 10^{-6}$ and 10^{-7}, however, it is the present SF-PNM which is

TABLE IX

Computing Times at Constant Accuracy for the Present SF-PNM and for the Numerov Method NM

Accuracy, ϵ, Eq. (57)	Time (sec)					
	The optic potential, Eqs. (41)–(42)			The Morse potential, Eqs. (43), (45)		
	t_{SF-PNM}	t_{NM}	$\frac{t_{NM}}{t_{SF-PNM}}$	t_{SF-PNM}	t_{NM}	$\frac{t_{NM}}{t_{SF-PNM}}$
10^{-3}	18.236	15.992	0.877	135.811	132.164	0.973
10^{-4}	32.327	29.580	0.915	289.467	229.129	0.792
10^{-5}	55.185	53.935	0.977	530.329	445.685	0.840
10^{-6}	105.092	107.532	1.023	963.975	896.147[b]	0.930
10^{-7}	184.144	184.966[a]	1.004	1656.043	D.P.[c]	—
10^{-8}	312.294	D.P.[c]	—	2643.776	D.P.[c]	—
10^{-9}	506.391	D.P.[c]	—	3303.167[d]	D.P.[c]	—

[a] The Numerov method was unable to yield e_{18} within this accuracy, see Fig. 2.
[b] The Numerov method was unable to yield e_{18} within this accuracy, see Fig. 4.
[c] The Numerov method requires double precision (D. P.) to yield this accuracy, see Figs. 2 and 4.
[d] In the case of the Morse potential, the available storage area on our computer CDC 3800 was exhausted before reaching this accuracy for the eigenvalues e_{17} and e_{18}, see Fig. 3.

somewhat faster even when imposing (52). For the Morse potential, which is rapidly varying at small r ($u(0) = 1669.6$, $u(1) = 12.6$, $u(2) = -188.4$, $u(4) = -79.8$, etc.), up to $\epsilon = 10^{-6}$, the Numerov method is faster than the present SF-PNM with the restriction (52). Nevertheless, the present SF-PNM is able to yield, in single precision, accuracies as high as (10^{-7}), 10^{-8}, or 10^{-9}, for which the Numerov method *requires double precision*. For this accuracy range, the Numerov method is about twice slower than the present SF-PNM. Of course, from the practical point of view, on the CDC computer, the single precision is quite enough even for the Numerov method. Thus, the use of one method or of the other (with constant step sizes (52)) is rather a matter of taste when a CDC computer is available. On an IBM computer, however, the situation changes seriously. Here, the Numerov method was not able to yield, in single precision, lines of constant accuracy better than $\epsilon = 10^{-4}$ for the optic potential, and $\epsilon = 10^{-2}$ for the Morse potential, whereas the present SF-PNM yielded lines of constant accuracy up to $\epsilon = 10^{-6}$. Thus, on IBM computers, the present SF-PNM should be preferred to the Numerov method.

We shall end with another feature which should be taken into account when comparing the two methods. The Numerov method is able to yield eigenfunctions at the mesh points only, whereas the SF-PNM is a *global method* [5], i.e., using the computed $y(r_{i-1})$ and $y'(r_{i-1})$, it provides us with an *analytic* approximation of the wavefunction on the ith interval. This feature was very well stressed by Gordon [6. 11]. It should be not minimized when comparing the relative merits of the various approaches to the numerical solution of (1).

APPENDIX: Taylor Series Expansions

All the quantities ξ_s, $s = 1, 2$, Eqs. (16), and ζ_p, $p = 0, 1,...,$ Eqs. (26) and (32), are finite as $\omega \to 0$. Indeed, in this case, power series expansions for these quantities give,

$$\xi_s(h) = \sum_{q=0}^{\infty} \frac{1}{(2q + s - 1)!} (\omega h)^{2q}, \qquad s = 1, 2,$$

$$\zeta_p(h) = \frac{(-1)^p}{2} \sum_{q=0}^{\infty} \frac{(q + p + 1)!}{q!\,(2q + 2p + 3)!} (\omega h)^{2q}, \qquad p = 0, 1, 2,....$$

Acknowledgments

Part of this work was accomplished during a period spent by one of the authors (Gh. A.) at the Department of Physics of the Condensed Matter, University of Geneva, Switzerland. He takes this opportunity for thanking the staff of the Department, and especially Professor M. Peter and Professor J. Sierro, Director, for kind hospitality and stimulating discussions. Valuable discussions with Dr. J. Piguet at the Computing Centre of the University of Geneva are also gratefully acknowledged.

The authors are indebted to the reviewers for the careful reading of the manuscript and for the many valuable suggestions they have formulated.

References

1. A. K. Bose, *Nuovo Cimento* **32** (1964), 379.
2. Gy. Bencze, Nordita Publications No. 184; *Comm. Phys. Math.* **31** (1966), 1.
3. R. G. Salvadori and M. L. Baron, "Numerical Methods in Engineering," Prentice-Hall, Englewood Cliffs, New Jersey, 1961.
4. B. L. Hulme, *Numer. Math.* **17** (1971), 367.
5. F. R. Loscalzo, Introduction to the Application of Spline Functions to Initial Value Problems, *in* "Theory and Application of Spline Functions" (T. N. E. Greville, Ed.), pp. 37–61. Academic Press, New York, 1969.

6. R. G. GORDON, *J. Chem. Phys.* **51** (1969), 14.
7. L. GR. IXARU, ICTP Trieste Int. Reports IC/69/6 and IC/69/7, 1969.
8. J. CANOSA AND R. G. DE OLIVEIRA, *J. Comput. Phys.* **5** (1970), 188.
9. GH. ADAM AND L. GR. IXARU, *Rev. Roum. Phys.* **20** (1975), 7.
10. J. P. RIEHL, D. J. DIESTLER, AND A. F. WAGNER, *J. Comput. Phys.* **15** (1974), 212.
11. R. G. GORDON, *in* "Methods in Computational Physics" (B. J. Alder, S. Fernbach, and M. Rotenberg, Eds.), Vol. 10, pp. 81–110. Academic Press, New York, 1971.
12. W. LEIGHTON, *J. Math. Anal. Appl.* **35** (1971), 381.
13. S. PRUESS, *SIAM J. Numer. Anal.* **10** (1973), 55.
14. L. GR. IXARU AND H. J. KREUZER, *Energ. Nucl.* **17** (1970), 61.
15. L. GR. IXARU, *Canad. J. Phys.* **49** (1971), 2947.
16. J. CANOSA, *J. Comput. Phys.* **7** (1971), 255.
17. W. LEIGHTON, *in* "Ordinary Differential Equations," pp. 497–501. Academic Press, New York, 1972.
18. A. C. ALLISON, *J. Comput. Phys.* **6** (1970), 378.
19. L. GR. IXARU, *J. Comput. Phys.* **9** (1972), 159.
20. R. L. TARP, Report UCRL–50430, Lawrence Radiation Laboratory, 1968.
21. L. GR. IXARU, *Rev. Roum. Phys.* **17** (1971), 7.
22. F. Y. HAJJ, H. KOBEISSE, AND N. R. NASSIF, *J. Comput. Phys.* **16** (1974), 150.
23. S. M. ROBERTS AND J. S. SHIPMAN, "Two-Point Boundary Value Problems: Shooting Methods," American Elsevier, New York, 1972.
24. L. FOX, "Numerical Solution of Ordinary and Partial Differential Equations," pp. 58–72. Pergamon Press, New York, 1962.
25. The method of the variation of the constants is the standard way for solving inhomogeneous linear differential equations. In connection with its use for the Schrödinger equation, see, e.g., D. ALPHARO AND T. REGGE, "Potential Scattering," Chap. 2. North–Holland, Amsterdam, 1965.
26. L. LAPIDUS AND J. H. SEINFELD, "Numerical Solution of Ordinary Differential Equations," Academic Press, New York, 1971.
27. P. MORSE, *Phys. Rev.* **34** (1929), 57.
28. L. D. LANDAU AND E. M. LIFSHITZ, "Quantum Mechanics, Non-Relativistic Theory," pp. 71–72. Pergamon Press, Oxford, 1965.
29. J. W. COOLEY, *Math. Comp.* **15** (1961), 363.
30. J. CANOSA, *J. Math. Phys.* **13** (1972), 615.